STUDIA UBB PHYSICA, Vol. 66 (LXVI), 1-2, 2021, pp. 121-131
(RECOMMENDED CITATION)
doi:10.24193/subbphys.2021.11

NONTHERMAL PLASMA IN CONTACT WITH LIQUIDS

S.D. ANGHEL[1]

ABSTRACT. The current work shows the generation methods of atmospheric pressure plasma in liquids or on liquids. The optical diagnosis proves the nonthermal character of generated plasmas. They were tested for dyes degradation, nanostructures synthesis and for obtaining of plasma activated water. The activated water preserves its new characteristics for at least three weeks and is a promising agent for bacterial inhibition.

Keywords*: in/on-liquid plasma, dye degradation, nanoparticles synthesis, plasma activated water, bacterial inhibition.*

INTRODUCTION

Although the gas discharges in liquids were known for many years due to their applications in various fields, during the last decades the non-thermal plasmas generated in liquids or in contact with liquids have been intensively investigated [1]. The researchers' attention was focused on two main directions: (a) plasma generation, plasma diagnostics and discharge mechanism clarification [2–4]; and (b) possible applications: decontamination, sterilization and purification processes [5–10], nanoparticles and polymers synthesis [11] and analytical spectrometry [12]. Generally, this kind of plasma is generated between two electrodes immersed in liquid or between an electrically powered electrode and a liquid which is in contact with a grounded electrode [1]. The voltage applied between electrodes can be continuous or time variable (sinusoidal or rectangular pulses, see Table 1). The ignition mechanism of plasma in liquids was most frequently related to the presence of gas bubbles in liquid. A gas can be bubbled into the liquid or gas micro-bubbles are the result of chemical and physical processes occurring in the liquid. When a bubble is very close to the powered electrode (mostly sharpened in order to create high electric fields), electric discharges like streamers or micro-arcs could be generated.

[1] *Babeș-Bolyai University, Faculty of Physics, 1 Kogălniceanu str., 400084 Cluj-Napoca, Romania*

Table 1. Electrode geometries for the generation of plasma in liquids.
Plasma gases: O_2, Ar, He, N_2, air.

Electrodes geometry	Ref.	Inter-electrode distance [mm]	Electrical parameters
tube-to-plate	[5]	5-10	pulse: 6 kV, 1 μs, 4.5 A_{pk}
plate-to-plate	[6]	10	pulse: 20 kV, 6 μs, 300 A_{pk}
	[7]	2-3	pulse: 8 kV, 0.2 μs, 4 A_{pk}
	[8]	0.5	DC: 0.7 kV, 40 mA
	[9]	7.5	pulse: 22 kV, 0.2 μs, 250 A
pin-to-plate	[3]	6	pulse: 15 kV, 2.5 μs, 1000 A_{pk}
multi pin-to-plate	[10]	10-15	DC high voltage
wire-to-cylinder	[13]	1 (quartz)	sinus, 13.56 MHz, 80 W

2. PLASMA GENERATION

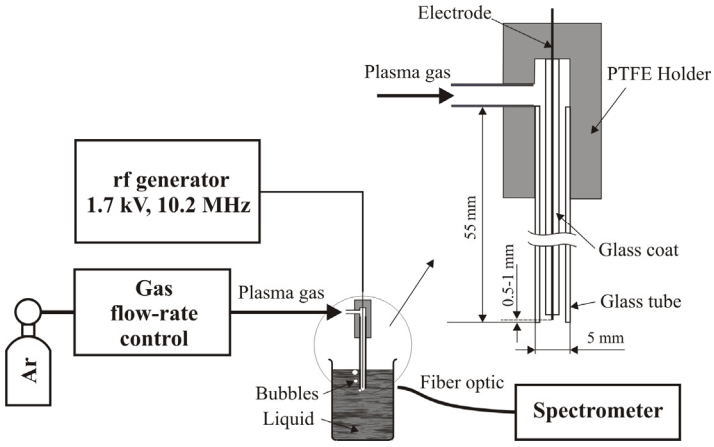

Fig. 1. The experimental set-up and a detail of the in-liquid plasma reactor.

Fig. 1 presents the schematics of the experimental set-up when plasma is generated in liqiud. The plasma reactor is composed of a metal wire electrode (Kanthal) placed via a holder piece in a quartz tube through which plasma gas flows with adjustable flow rate. The electrode is powered with high sinusoidal voltage generated with a laboratory made free-running oscillator [14]. The glass tube is vertically immersed in the liquid at a depth of 15-20 mm. When plasma gas (argon) flows, at the immersed exit of the glass tube gas bubbles arise with a cadency (0.5 – 10 bubbles/second) which depends on the gas flow rate (0.06 –

0.35 l min^{-1}). During each bubble life a glow discharge is generated between the free end of the electrode and the bubble wall. Fig. 2 shows the most representative video frames from the point of view of the discharge dynamics. A discharge cycle has three stages: (1) pushing the water towards the end of the quartz tube and the gas bubble formation, frames 1-38; (2) the discharge initiation at the powered electrode and its development as streamers with many branches bridging the electrode and the gas-water wall. Simultaneously the gas bubble expands outside the glass tube, frames 43-54; and (c) the extinction of the discharge when the gas bubble detaches from the border of the quartz tube and slides up on its wall, frames 55-57.

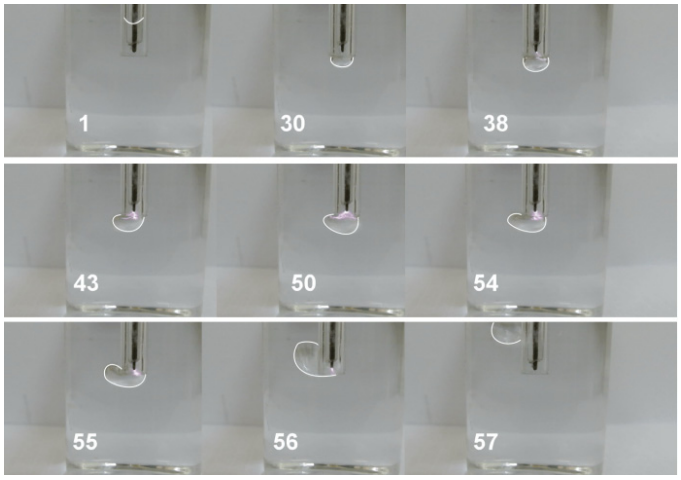

Fig. 2. Time evolution of the plasma generation process during an ignition-extinction cycle. Each imprinted number indicates the number of the frame from a total of a 63 frames/cycle.

The experimental setup to generate plasma on liquid presented in Fig. 3 is very similar to the one presented in Fig. 1, excepting the discharge reactor. It was replaced with two different powered electrodes for generating the plasma on water. The first one is a capillary metallic tube through which helium or argon flows to generate a plasma μ-jet surrounded by the ambient atmosphere. To generate a μ-arc discharge in ambient air a Kanthal wire electrode was used. The second electrode for both discharges is represented by the treated water. The inserts from Fig. 3 show the μ-jet and μ-arc discharges.

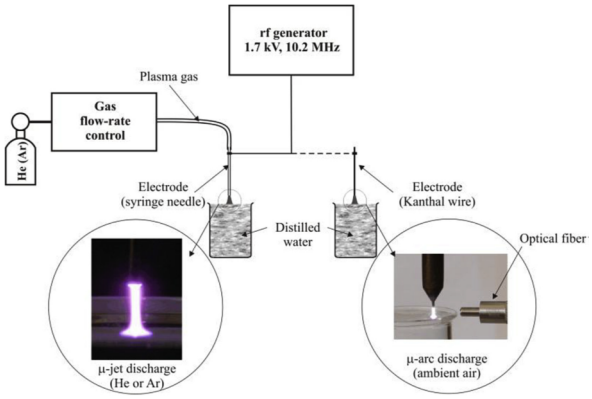

Fig. 3. Experimental set-up to generate plasma on liquid.

3. RESULTS AND DISCUSSION [15 - 20]

3.1 Plasma emission

Fig. 4 shows the emission spectrum of Ar plasma generated in distilled water. With the exception of the argon emission lines, the emission lines of hydrogen (H_α) and oxygen, and the emission bands of $OH^\bullet$ radical as a result of water molecules dissociation are present. Based on the spectrum, plasma parameters were determined: T_{excAr} = 6080 K, T_{rotOH} = 1990 K and n_e = $3.79 \cdot 10^{15}$ cm^{-3}. The high excitation temperature of the electrons in Ar atoms indicates the presence of energetic electrons capable of generating**,** by inelastic collisions, molecular species able to degrade organic dyes, mainly hydroxyl radical $OH^\bullet$ with a high oxidation character.

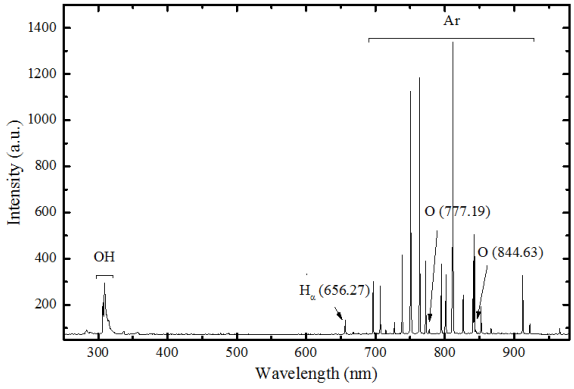

Fig. 4. Emission spectrum of plasma generated in Ar bubbled in water.

3.2 Methylene blue degradation with in-liquid plasma and time evolution of the solution characteristics

Being known that the main degradation mechanisms of MB solutions is the decomposition by energetic electrons and the oxidation under the action of hydroxyl radical and hydrogen peroxide, the influence of the initial dye concentration and the treatment time on the degradation process and on the time evolution of the MB solutions' characteristics after the ending of the exposure to plasma were studied.

The gradual change of the UV-vis spectra and of the visual aspect (see the insertion) for the solution containing 100 mg l^{-1} MB is exemplified in Fig. 5.

The spectra show the characteristic absorption bands of MB in water. The exposure to plasma treatment produces changes in the absorption spectrum. The main absorption band (663 nm) decreases in intensity, a blue shift is observed and after 45 minutes it becomes a flat line suggesting that the methylene blue solution was completely discolored. The blue-shift of the 663 nm band might be correlated to the change of pH which decreases from a value of 5 before treatment, to the value of 2 after the complete degradation. This might be due to the formation of intermediate organic acids during the degradation process of the MB molecules but more importantly due to H^+ produced by means of water dissociation.

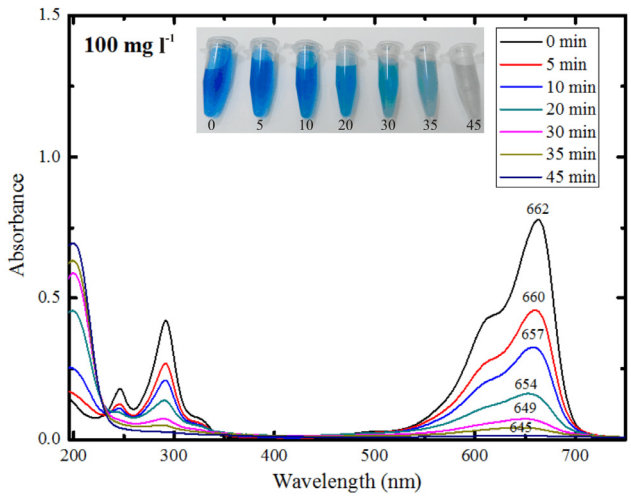

Fig. 5. The absorption spectra evolution for the MB solution with an initial concentration of 100 mg l^{-1} and the image of the samples collected during plasma treatment at different time intervals after the beginning of the treatment.

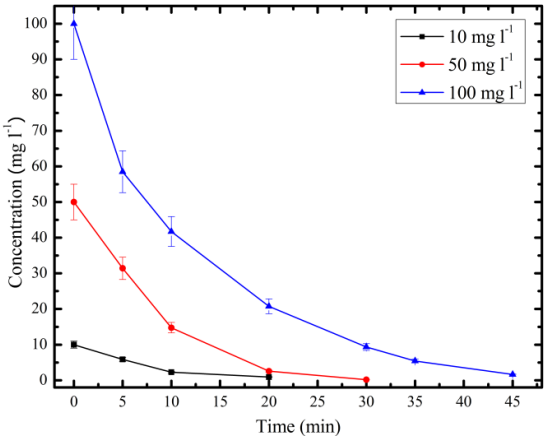

Fig. 6. The dependence of the MB concentration on the treatment time with the initial concentration as parameter.

The changes in MB concentration during the plasma treatment are presented in Fig. 6. The time evolution of the MB concentration shows that the degradation process continues slowly for at least ten minutes even after the plasma treatment was stopped. This fact suggests that the active species generated by the plasma are the ones responsible for the degradation.

During the plasma treatment the electrical conductivity of MB solution increases relatively linear from very low values to higher ones as it can be seen in Table 2. The increase in the electrical conductivity leads to suppose that new ions are generated at the plasma-liquid interface by water molecules dissociation and these ions are H^+. The values of the electrical conductivity and pH after two weeks from the treatment suggest that the processes are irreversible at least for this time period.

Table 2. The time evolution of the electrical conductivity and pH of the treated MB aqueous solution (50 mg l^{-1}, 35 min treatment time)

Electrical conductivity, µs cm^{-1}			pH		
Before treatment	At the end of treatment	Two weeks later	Before treatment	At the end of treatment	Two weeks later
9	595	635	5	4	3

3.4 Carbon structures synthesis with in-liquid plasma

Concurrently with the MB degradation a secondary result of the treatment with plasma which was not mentioned so far in papers, is the progressive generation of very small solid structures. The XPS analysis shows that the plasma breaks the structure and seems to favor the bonding of oxygen in different molecular sites leading to the formation of new bonds of the oxygen with carbon and even nitrogen and sulfur. Thus we could explain the formation of the very small solid particles which are formed preponderantly of carbon and also of contributions coming from oxygen. The TEM image, shown in Fig. 7, reveals the presence of spherical particles having tens of nm in diameter in these solid structures. The insertion from figure 7 shows a great number of solid structures obtained after 45 minutes of treatment of the solution with a concentration of 100 mg l^{-1} MB.

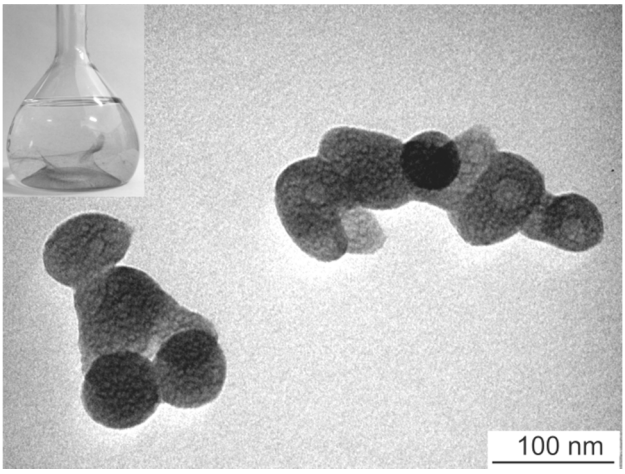

Fig. 7. TEM image of solid structures generated by treatment with bubbled Ar plasma of 100 mg l^{-1} MB solution. The insert presents a photo of the solid particles in solution at the end of the plasma treatment.

A schematic representation of the synthesis procedure is presented in Fig. 8. It suggests that there are three main mechanisms for dye degradation in plasma in liquids: electron bombardment, ion collision and radical induced degradation. It also shows that the nature of plasma gas (Ar or He) influences the dimensions and forms of the synthesised carbon nanostuctures.

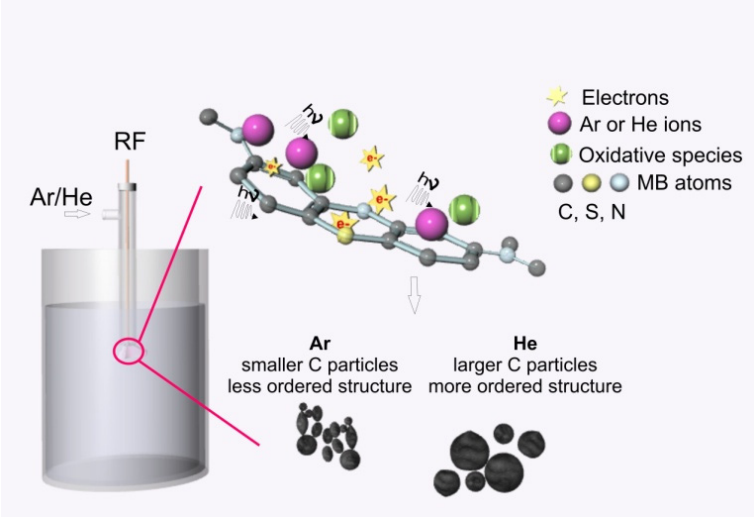

Fig. 8. Schematic representation of the synthesis procedure and mechanism.

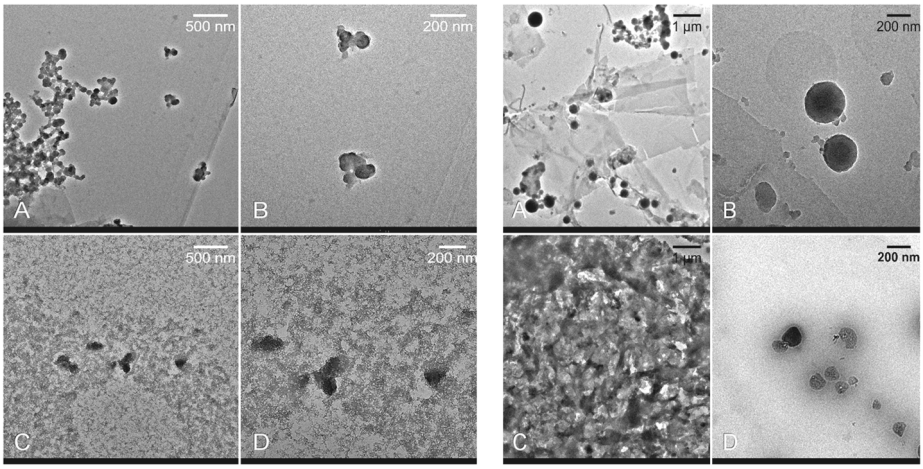

Fig. 9. TEM images of the Ar plasma carbon structures (left) obtained at different time treatments: A,B-20 minutes C,D- 40 minutes and of the He plasma carbon structures (right) obtained at different time treatments: A,B-20 minutes C,D- 60 minutes.

The TEM analysis (Fig. 9) showed that the structures obtained with the He plasma are larger compared to the case of the Ar plasma and revealed that the plasma has a destructive effect on the structures as well.

3.5 Plasma activated water and bacterial inhibition

Under the action of atmospheric pressure plasma, distilled water changes its characteristics, mainly pH and electric conductivity, and acquire an important oxidative potential. The so treated water is named plasma activated water (PAW). Depending on the nature of the discharge gas (Ar, He, O_2, air, or their mixture), reactive oxygen species (ozone O_3, hydrogen peroxide H_2O_2, hydroxyl radical $^{\cdot}OH$) and reactive nitrogen species (peroxynitrite, nitrate, nitrite and the corresponding acids, nitrogen oxides NO_x) are generated in the plasma core or in the plasma-liquid contact zone being then dissolved in the liquid. Fig. 10 shows the dependence of their concentrations on the treatment time. They are responsible for a large variety of applications of plasmas in contact with liquids, mainly in the bio-medicine field and for reduction of environmental pollution. The presence of nitrogen is important for the activation of water-based liquids. Generally, it enters in the discharge from ambient air as a result of diffusion and contributes to the generation in plasma of reactive oxygen and nitrogen species which are then transferred to the liquid phase.

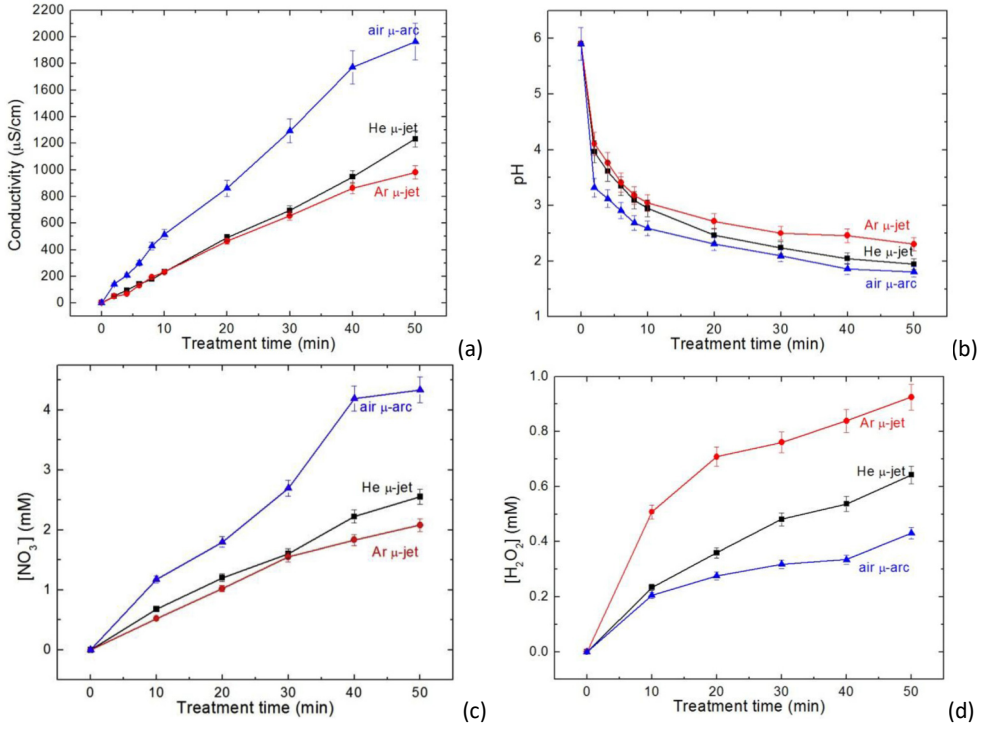

Fig. 10. Electrical conductivity (a), pH (b), nitrate (c) and H_2O_2 (d) concentrations dependences on the treatment time for water samples of 35 ml.

The new attributes (pH value, electrical conductivity, nitrate and hydrogen peroxide concentrations) acquired by the PAW solutions do not change significantly for at least 21 days.

The so obtaned PAW's were used to study the inhibitory effect on *Staphylococcus aureus*. The bacteria was selected because it is one of the most common infectious agents as it causes numerous skin and respiratory infections, food poisoning and it is very dangerous in hospital hygiene. The PAW's were incubated with the microorganisms and their inhibition effect on the bacteria is assessed. The inhibition effect was investigated by determining the optical density of the bacterial suspensions at 620 nm using a Jasco V-530 UV-VIS spectrophotometer. It was estimated as it is shown in [20].

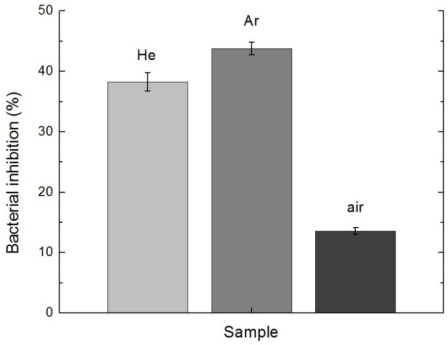

Fig. 11. Bacterial inhibition effect of PAW – discharge type influence.
PAW obtained after exposure to the plasmas for 50 minutes was used.

Fig. 11 shows that the air discharge offers the lowest inhibition rate while the Ar discharge shows the more intense effect. Considering the properties of the PAW ilustrated in Fig.10, it can be observed that the Ar discharge creates the highest concentration of hydrogen peroxide, followed by the helium and air discharges, which is similar to the inhibition effect on the *S.aureus* samples. Furthermore, by increasing the treatment time of the PAW samples, the concentration of hydrogen peroxide is also increased.

CONCLUSIONS

This work has shown the possibility to generate plasma in liquids by using a new device for bubbling the plasma gas and atmospheric pressure plasma on liquids. The plasma emission shows the presence of chemically active species which

are important for methylene blue degradation and for synthesis of carbon based nanoparticles. The activation of distilled water was also studied. Plasma activated water has a long time stability and represents a promising agent for bacterial inhibition.

AKNOWLEDGEMENTS

The author thanks to Dr. Iulia Elena Vlad and Dr. Diana Zaharie-Butucel for successful collaboration over several years.

REFERENCES

1. P. Bruggeman, C. Leys, *J. Phys. D: Appl. Phys*., 42, 053001 (2009).
2. Q. Chen, J. Li, K. Saito, H. Shirai, *J. Phys. D: Appl. Phys.,* 41, 175212 (2008).
3. P. Vanraes, A. Nikiforov, C. Leys, *J. Phys. D: Appl. Phys.*, 45, 245206 (2012).
4. P. Bruggeman, J, Degroote, C. Leys. J. Vierendeels, *J. Phys. D: Appl. Phys*., 41, 194007 (2008).
5. S. Gershman, O. Mozgina, A. Belkind, K. Becker, E. Kunhardt, *Contrib. Plasma Phys.,* 47 19 (2007).
6. K. Sato, K. Yasuoka, S. Ishii, *Electr. Eng. Jpn*., 170, 1 (2010).
7. K. Yasuoka, K. Sato, *Int. J. Plasma Env. Sci. Technol.,* 3, 22 (2009).
8. [19] A. Yamatake, H. Katayama, K. Yasuoka, S. Ishii, *Int. J. Plasma Env. Sci. Technol.,* 1, 91 (2007).
9.T. Miichi, N. Hayashi, S. Ihara, S. Satoh, C. Yababe, *Ozone-Sci. Eng*., 24, 471 (2002).
10. Y. Akishev, M. Grushin, V. Karalnik, N. Trushkin, V. Kholodenko, V. Chugunov, E. Kobzev, N. Zhirkova, I. Irkhina, Kireev G, *Pure Appl. Chem.,* 80, 1953 (2008).
11. D. Mariotti, R. M. Sankaran, *J. Phys. D: Appl. Phys.,* 44, 174023 (2011).
12. P. Jamroz, P. Pohl, W. Zyrnicki, *J. Anal. Atom. Spectrom.,* 27, 1032 (2012).
13. H. Aoki, K. Kitano, S. Hamaguchi, *Plasma Sources Sci. Technol.,* 17, 025006 (2008).
14. S. D. Anghel, *IEEE Trans. Plasma Sci.,* 30, 660 (2002).
15. S. D. Anghel, D. Zaharie-Butucel, I. E. Vlad, *J. Electrostat.*, 75, 63 (2015).
16. D. Zaharie-Butucel and S.D. Anghel, *Roum. Journ. Phys.,* 59, 757 (2014).
17. I. E. Vlad, O. T. Marisca, A. Vulpoi, S. Simon, N. Leopold and S. D. Anghel, *J. Nanopart. Res.,* 16, 2633 (2014).
18. D. Zaharie-Butucel, J. Papp, C. Leordean, S. D. Anghel, *RSC Advances,* 5, 98325 (2015).
19. I. E. Vlad, S. D. Anghel, *J. Electrostat.,* 87, 284 (2017).
20. I. E. Vlad, C. Martin, A.R. Toth, J. Papp, S. D. Anghel*, Rom. Rep. Phys.,* 71, 602 (2019).